

1 Article

2 Inter- and intra-host nucleotide variations in hepatitis

3 A virus in culture and clinical samples detected by

4 next-generation sequencing

5 **Zhihui Yang^{1*}, Mark Mammel¹, Chris A. Whitehouse², Diana Ngo¹, Michael Kulka¹**6 ¹Office of Applied Research and Safety Assessment, Center for Food Safety and Applied Nutrition, U.S. Food
7 and Drug Administration, Laurel, Maryland, 207088 ²Office of Research, Center for Veterinary Medicine, U.S. Food and Drug Administration, Laurel, Maryland,
9 2070810 *Correspondence: Zhihui.yang@fda.hhs.gov; Tel: 1-301-796-0641

11

12 **Abstract:** The accurate virus detection, strain discrimination, and source attribution of contaminated
13 food items remains a persistent challenge because of the high mutation rates anticipated to occur in
14 foodborne RNA viruses, such as Hepatitis A virus (HAV). This has led to predictions of the existence
15 of more than one sequence variant between the hosts (inter-host) or within an individual host (intra-
16 host). However, there have been no reports of intra-host variants from an infected single individual,
17 and little is known about the accuracy of the single nucleotide variations (SNVs) calling with various
18 methods. In this study, the presence and identity of viral SNVs, either between HAV clinical
19 specimens or among a series of samples derived from HAV clone1-infected FRhK4 cells, were
20 determined following analyses of nucleotide sequences generated using next-generation
21 sequencing (NGS) and pyrosequencing methods. The results demonstrate the co-existence of inter-
22 and intra-host variants both in the clinical specimens and the cultured samples. The discovery and
23 confirmation of multi-viral RNAs in an infected individual is dependent on the strain discrimination
24 at the SNV level, and critical for successful outbreak traceback and source attribution investigations.
25 The detection of SNVs in a time series of HAV infected FRhK4 cells improved our understanding
26 on the mutation dynamics determined probably by different selective pressures. Additionally, it
27 demonstrated that NGS could potentially provide a valuable investigative approach toward SNV
28 detection and identification for other RNA viruses.

29 **Keywords:** inter- and intra-host nucleotide variations, Hepatitis A virus, next-generation
30 sequencing, pyrosequencing

32 1. Introduction

33 The majority of the known foodborne viruses, either linked or found directly responsible for
34 foodborne illness, have RNA genomes [1]. RNA viruses have been shown to exhibit high mutation
35 rates primarily due to the low-fidelity of RNA polymerases [2] and absence of post-replication
36 nucleotide repair mechanisms [3, 4]. Therefore, these RNA viruses are generally expected to exist as
37 populations of non-identical but closely genetic-related viral variants between the hosts (inter-host)
38 or within an individual host (intra-host), which are referred to as quasispecies [5, 6]. Viral genetic
39 heterogeneity, generated by single nucleotide variations (SNVs), is believed to be a strategy of virus
40 evolution and virus adaptability [4]. However, the presence of more than one sequence variant is a

41 challenge for accurate virus detection, identification, and source attribution of contaminated food
42 items.

43 Hepatitis A virus (HAV) is one of the identified major foodborne viruses in the U.S. [1, 7].
44 Although the incidence of HAV has declined due to the introduction of HAV vaccines in the 1990's
45 [8, 9], the number of cases appears to be increasing in the U.S. (estimated number of new HAV
46 infection in 2015 was 2800, according to the CDC: Viral Hepatitis Surveillance United States, 2015),
47 as well as around the world (estimated number of HAV clinical cases was 1.5 million, according to
48 the World Health Organization, 2000). HAV is commonly transmitted person-to-person, or through
49 the consumption of contaminated food or water, and large outbreaks of HAV associated with
50 contaminated food continue to be reported worldwide [10-13].

51 HAV is a non-enveloped, RNA virus belonging to the family Picornaviridae, whose single-
52 stranded genome of approximately 7.5 kilobases (kb) in length, contains a single open reading frame
53 encoding a single polyprotein flanked by 5' and 3' untranslated regions, as well as a 3' poly(A) tail
54 [14, 15]. Since its discovery in 1973 by Steven Feinstone [16], HAV has evolved through nucleotide
55 mutations and recombination and is classified into three genogroups among which the nucleotide
56 variation is more than 15% [17]. Traditionally, a highly variable region of 168 nucleotides within the
57 viral genome encoding the VP1/P2A junction has been used for identifying and discriminating
58 between different HAV strains [18]. However, several alternative regions within the genome
59 including those encoding for VP1, 2C and 3D also display high nucleotide variability and have
60 offered limited alternative regions for strain identification [19]. Thus, whether tracking HAV strain(s)
61 as they circulate through a given population or region, or linking a contaminated food item to an
62 outbreak of illness, it is necessary and critical to accurately identify HAV strains by as few as one
63 nucleotide variation along the entire viral genome. Whole genome sequencing (WGS) offers an
64 approach by which single nucleotide differences/variations may be identified among strains. Inter-
65 host HAV variants have been reported either under laboratory conditions or from clinical samples
66 [20-22]. Vaughan *et al.* [23] completed the WGS analysis on HAV constructed from 16 PCR amplicons
67 of 101 HAV strains as serum specimens from 4 food-borne outbreaks and 14 non-outbreaks. The
68 whole genome data showed inter-host genetic diversity among the outbreaks and cases; however,
69 analysis of intra-host HAV variants from eight patients of the same outbreak showed only a single
70 sequence variant. In other words, intra-host variation was not commonly observed, which is likely
71 due to the stringent negative selection preventing accumulation of SNVs during HAV infection [3].

72 Our previous study on HAV clone1-infected FRhK4 cells showed that both inter- and intra-host
73 variants of only one single nucleotide difference existed in the absence of immune selection [24].
74 Although WGS offers the opportunity for accurate tracking of HAV strains and attributing the
75 contamination sources, there have been no reports of intra-host variants from one infected single
76 individual, and little is known about the accuracy of SNV calling with various methods, including
77 pyrosequencing and next-generation sequencing (NGS). This study extends our previous
78 investigative approach to the identification and discrimination of intra- and inter-host HAV variants
79 from both cultured and clinical samples. We examined the relationship between the frequency of
80 SNVs identified by NGS and the pyrosequencing confirmation by presenting a working model for
81 HAV SNV calling from NGS data.

82 2. Materials and Methods

83 *Viruses, cell culture and clinical samples*

84 The virus HAV/HM175 clone 1 is a cell culture-adapted strain of wild-type HAV/HM175
85 purchased from ATCC (VR-2089). Fetal rhesus monkey kidney FRhK-4 cell line persistently infected
86 with clone 1 (defined as F4-c1 in this study) was established and maintained in our lab following the
87 protocol previously described [25-27]. Persistently infected cells were sub-cultured in MEM-
88 GlutaMax (GIBCO) supplemented with 1% pyruvate, 1% non-essential amino acids (GIBCO) and 5%
89 heat-inactivated fetal bovine serum at 37°C, and split at a ratio between 1:30 to 1:40, sufficient to yield
90 a confluent culture weekly. The cells were periodically collected from 62 to 1200 days post-infection

91 (dpi) and used for this investigation. The HAV HM175 positive human stool sample was obtained
92 from Dr. Suzanne Emerson (National Institutes of Health).

93 *Sample preparation, RNA isolation and viral RNA quantification by RT-PCR (RT-qPCR)*

94 F4-c1 cells were harvested at 100% confluence at different time points (62, 120, 180, 240, 335, 417,
95 500, 600, 800, 996 and 1200 dpi) as previously described [24, 25]. In brief, cells were harvested from a
96 T225 flask by scraping in culture medium, centrifuged at 1500 \times g for 30 min at 4°C, cell pellets were
97 washed and re-suspended in 2.5 mL cold phosphate-buffered saline (PBS) for subsequent use. Prior
98 to RNA (termed as F4-C1 RNA in this study) isolation, cell pellets from each time point were lysed
99 by subjecting to three rounds of freeze/thaw using a dry ice/methanol bath and a room temperature
100 water bath, respectively. Complete disruption of cell integrity was determined by microscopic
101 examination of a 1:1 dilution of the lysate in 0.4% trypan blue buffered solution (Gibco). Viral RNA
102 was isolated from the F4-c1 cell lysates, or HM175 stool supernatant in 10% PBS (vol/vol),
103 respectively, with the QIAamp Viral RNA mini kit (Qiagen) following the manufacturer's protocol.
104 To determine the HAV genome copy numbers in the samples, one-step RT-qPCR was carried out
105 following the protocol previously published [1, 24]. In brief, all RNA samples were analyzed in
106 replicates using QuantiTect Probe RT-PCR kit (Qiagen) with a 25 μ L reaction volume containing 5
107 μ L RNA. Ten-fold serial dilutions of a RNA transcript containing a complete HAV genome sequence
108 generated from pHAV/7.1 as described previously by Yang et al. [24] were used to generate standard
109 curves (RNA copy versus Ct). The reaction program included reverse transcription of RNA at 50 °C
110 for 30 min, followed by a denaturation at 95 °C for 15 min, and finally 45 cycles of amplification (10 s
111 at 95 °C, 25 s at 53 °C, and 25 s at 72 °C).

112 *Library generation and sequencing*

113 Double stranded cDNA libraries were generated from all the RNA samples above using a
114 TruSeq stranded mRNA prep kit (Illumina) following our previously published protocol [1, 24]. The
115 total RNA input of each F4-C1 sample ranged from 1 – 3 μ g. The viral RNA input from the HM175
116 stool sample was 8.4x10⁸ copies. The libraries were validated for quality control by using the
117 TapeStation (Agilent), and for quantification by using Qubit (Thermo Fisher). Barcoded libraries were
118 pooled and sequenced on the MiSeq platform (Illumina) generating paired-end 100 base pairs (bp)
119 reads.

120 *De novo assembly and reference-based mapping*

121 The raw read data in FASTQ files of all samples was imported from MiSeq into the CLC Genome
122 Workbench v9.0 (CLC Bio), and sequence quality was determined before further analysis. For the
123 samples in which the SNVs were investigated by both NGS and pyrosequencing, reference-based
124 mapping was performed on the reads from the HM175 stool sample against the complete genome
125 sequence of wild-type HAV HM175 (GenBank accession number M14707), and on the reads from 62
126 to 240 dpi samples against the HAV HM175/clone 1 sequence in NCBI (GenBank accession number
127 M16632). Reads from the F4-c1 62 dpi sample (the earliest time point available in this study) were
128 trimmed and *de novo* assembled to generate the viral genome using default parameters. The
129 assembled contig was 7,474 nt in length and showed a 99% identity with the complete genome of
130 HAV (attenuated) RNA (GenBank accession number M16632) as BLAST'd against the NCBI database.
131 For the F4-c1 samples in which the SNVs were only investigated by NGS, this contig at 62 dpi was
132 taken as the reference sequence, reference-based mapping was carried out on the reads of each
133 sample from the time points afterward. In addition, the mapping parameters used had an 80%
134 similarity over 50% of the read length as default. Total reads and mapped reads were summarized,
135 and an estimated coverage was calculated to evaluate the overall coverage of the viral genome for
136 each sample.

137 *Single nucleotide variation calling from NGS reads and confirmation by pyrosequencing*

138 Single nucleotide variation calling was carried out on each viral read mapping in CLC Genomics
139 WorkBench. Since the estimated sequencing error rate with Illumina platform is approximated 2%
140 [28, 29], to ensure high-quality and reliable variant calling, the parameters were set as minimum
141 coverage of 10, and minimum frequency of 2%. To confirm the SNV detected by NGS,
142 pyrosequencing was performed on some of the samples (62 to 240 dpi F1-C1 RNA, HM175 stool

143 RNA) following the protocol previously published [24, 30, 31]. First, reverse transcription with
144 oligo(dT) primer (Promega) was carried out on the viral RNA samples to generate cDNA. Second,
145 PCR with flanking primers (Supplementary table 1a) was performed to amplify the amplicons
146 ranging from 148 to 553 bp in length to cover the genomic regions of interest. Third, pyrosequencing
147 was carried out by annealing the amplicons to the sequencing primers (Supplementary table 1b), then
148 biotinylated and immobilized onto streptavidin-coated Sepharose beads in a 96-well plate. Finally,
149 specific nucleotides were added to the sequencing-primer-bound ssDNA, and the light signal
150 associated with the identity of the incorporated nucleotides was recorded.

151 *GenBank accession number*

152 The data from Illumina sequencing have been deposited in the NCBI Sequence Read Archive
153 (www.ncbi.nlm.nih.gov/sra) under accession number SRP118687 (BioProject PRJNA408289).

154 **3. Results**

155 Our previous study revealed that an intra-host heterogeneity existed in virus-infected cultured
156 cells detected by NGS and was confirmed with pyrosequencing [24]. Pyrosequencing methods are
157 well-established and have proven suitable for SNV analysis and viral SNV identification [32, 33];
158 this technology is capable of detecting and quantifying allelic frequency to as low as ~5% [34]. We
159 also concluded in our previous study that both read coverage and nucleotide frequency at a given
160 position are significant for the SNV calling from NGS data and pyrosequencing confirmation [24].
161 The requirement of sequencing coverage varies and depends on the specific applications. For
162 example, in determining the sequence variation of SNVs and small indels (insertions and deletions),
163 it usually requires an average depth of 15x and 33x to detect homozygous SNVs and the same
164 proportion of heterozygous SNVs, respectively, based on the studies on human genome sequencing
165 with the Illumina platform [35, 36]. Consequently, an average coverage depth of 50x was suggested
166 for the requirement to allow reliable SNV calling along 95% of the genome [37]. In the current
167 investigation, each of the SNVs selected for confirmation by pyrosequencing had a relatively high
168 depth of nucleotide coverage ($\geq 93x$, data not shown) and high base quality (Phred quality score > 30 ,
169 or the base call accuracy $> 99.9\%$), thus, the results in this study showed mainly the relationship
170 between SNV frequency from NGS and the SNV validation with pyrosequencing.

171 We first sought to determine whether intra-host variation(s) exist in HAV from clinical samples.
172 Illumina MiSeq reads from a HAV/HM175 positive stool sample were mapped against the wild-type
173 HM175 reference sequence (GenBank accession number M14707); eight SNVs were detected with
174 frequencies ranging from 13.8 – 99.7%. The depth of the read coverage at each nucleotide position
175 was $\geq 24,000x$ (Table 1). These SNVs were identified by the NGS variant caller as either “single-SNV”
176 or “mixed-SNVs”. In the case of single-stranded genomes such as HAV, “single-SNV” is defined as
177 having only one major variant called at that position, and “mixed-SNVs” is defined as having more
178 than one variant called at that position. To validate the SNVs called from NGS, pyrosequencing was
179 carried out on all eight SNVs. The SNVs at positions 2864, 4185, 5204, 6216 and 6522 had variant
180 frequencies ranging from 81.1 – 99.7 and were all confirmed as single-SNV (i.e., inter-host variations)
181 by pyrosequencing (Table 1). In contrast, two of these five SNVs (at positions 5204 and 6216) were
182 called by NGS as “mixed-SNVs”. On the other hand, SNVs at positions 1742 and 6836 with
183 frequencies of 54.2 and 40.1 were both called and confirmed as mixed-SNVs and therefore represent
184 intra-host variations (Supplementary figure 1). The insertion at 7042 with a frequency of 13.8 was not
185 confirmed as a real SNV by pyrosequencing.

186

187 **Table 1.** Identification of SNVs present in viral RNA extracted from a HAV/HM175 positive stool
188 sample.

Reference Position ^a	Coding Region	Reference ^b	Change ^c	Coverage ^d	Frequency ^e	SNV called by NGS ^f	Amino acid change ^g	SNV identified by pyrosequencing
1742	1C	G	A	22779	54.2	mixed		mixed
2864	1D	T	A	24773	99.3	single		single
4185	2C	G	A	69820	99.7	single	AAA45465.1:p.[Glu1151Lys]	single
5204	3A	G	A	138614	81.1	mixed		single
6216	3D	T	C	166496	81.7	mixed		single
6522	3D	T	A	297276	99.6	single	AAA45465.1:p.[Ser1930Thr]	single
6836	3D	C	T	210792	40.1	mixed		mixed
7042	3D	-	A	260563	13.8	mixed	AAA45465.1:p.[Gln2103fs]	Non-SNV

189 ^a Nucleotide position in reference sequence M14707.

190 ^b The reference sequence at the position of the variant.

191 ^c The changed sequence of the variant.

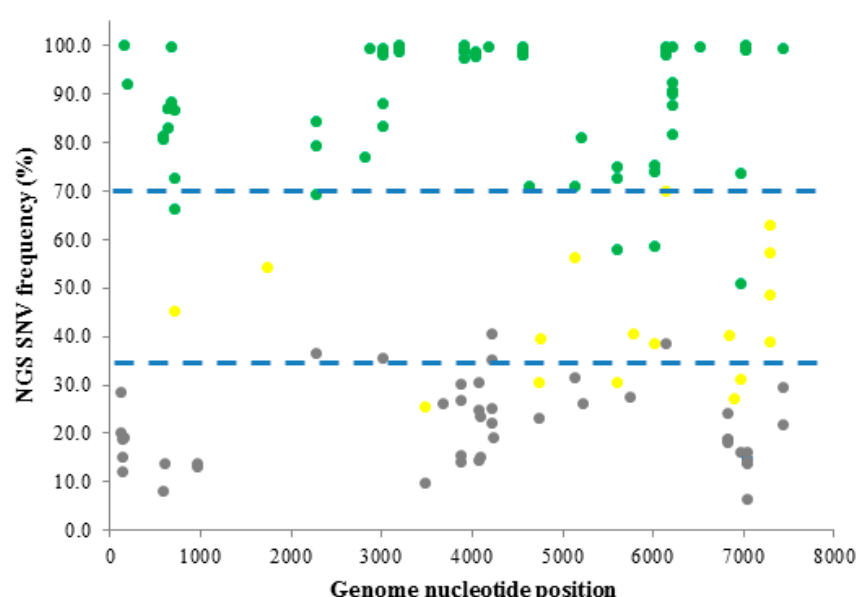
192 ^d The depth of NGS coverage at that nucleotide position.

193 ^e The read count of variant at that nucleotide position divided by coverage.

194 ^f The SNVs called at this position by the variant caller. Single-SNV: only one variant called at
195 that position; mixed-SNV: more than one variant called at that position.

196 ^g Amino acid change in the coding region of the hepatitis A virus polyprotein AAA45465.1.

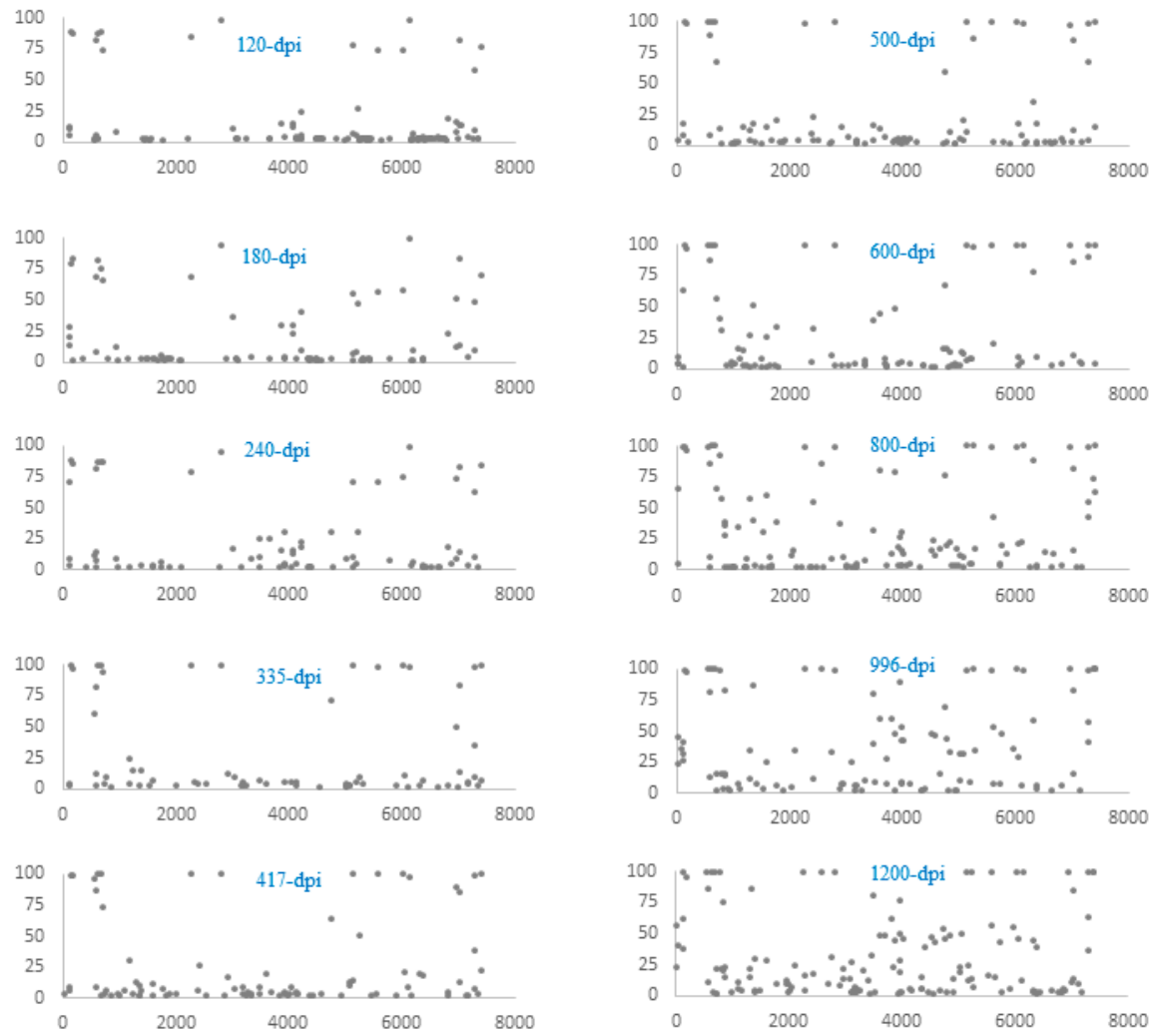
197 To investigate the relationship between the frequency of SNV calling from NGS and the confirmation
198 of SNVs with pyrosequencing, first, NGS was performed and SNVs were called on the clinical sample
199 (against reference M14707), and cultured F4-c1 samples at time points of 62 to 240 dpi ((against
200 reference M16632). One hundred and thirty-four SNVs with the average coverage ranged from 93 –
201 5324x were detected by NGS (Figure 1). Pyrosequencing was then performed on each of these SNVs.
202 Seventy-one SNVs were identified by pyrosequencing as single-SNVs, and 66 (93.0%) of them had
203 NGS frequencies ranging from 70.9 to 100%; 17 SNVs were identified as mixed-SNVs, and 12 (70.6%)
204 of them had frequencies ranging from 35.2 to 69.9%; 46 SNVs were not validated by pyrosequencing,
205 and 41 (89.1%) of them had frequencies ranging from 6.3 to 33.5%. Thus, based on our current data
206 and graphical analysis (Figure 1), a SNV from NGS with a frequency >70% could be validated by
207 pyrosequencing as a single-SNV with a 93.0% probability; a SNV from NGS with a frequency between
208 35-70% could be validated by pyrosequencing as a mixed-SNVs with a 70.6% probability; however,
209 if a SNV called by NGS has a frequency < 35%, then there is an 89.1% possibility it would not be
210 validated as a real SNV by pyrosequencing. We used this relationship as a model to predict the single-
211 SNV, mixed-SNVs, and non-SNVs in the following experiments based on their NGS frequencies.



216

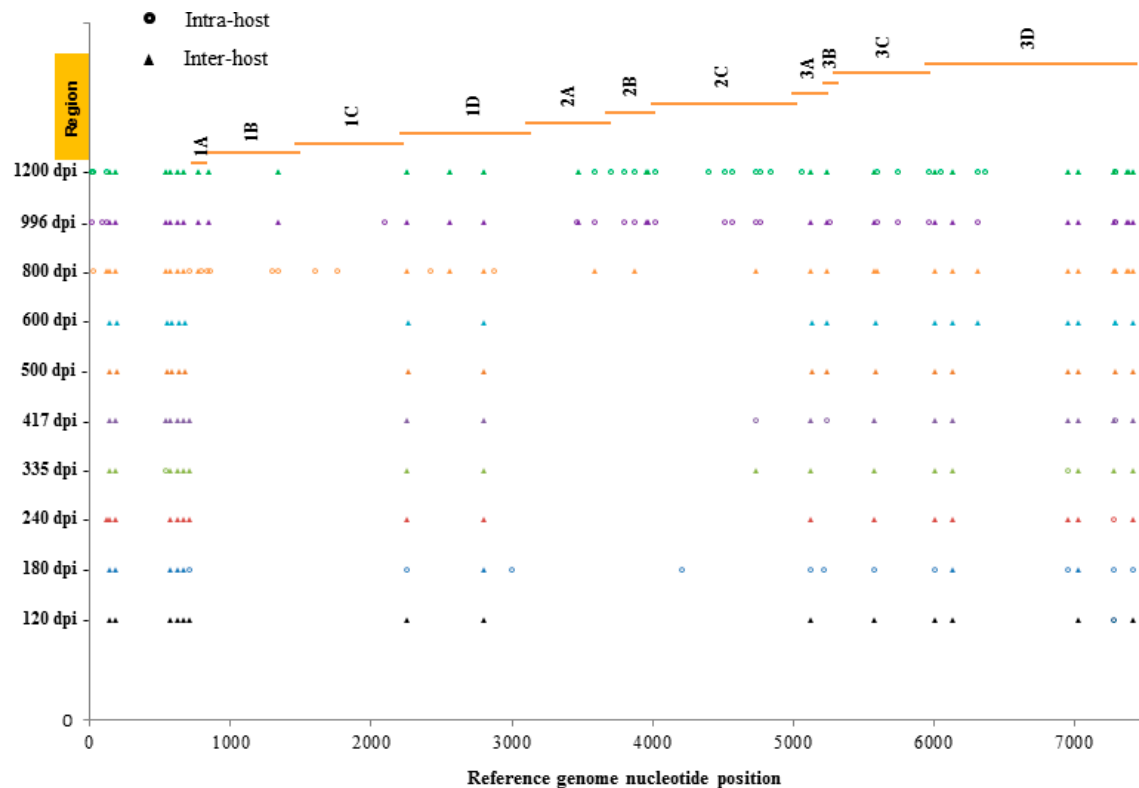
217 **Figure 1. Comparison of SNV calling between NGS and pyrosequencing.** Each dot represents
218 an individual SNV identified by NGS in extracts from either F4-c1 culture (62 to 240 dpi) against the
219 reference sequences M16632, or the HAV/HM175 positive clinical sample against the reference
220 sequence M14707. Phred quality score >30 for each SNV ($p<0.001$ for the error rate). SNVs were
221 validated by pyrosequencing as a single-SNV (green), mixed-SNVs (yellow), or a non-SNV (grey).
222 The dotted blue lines were artificially drawn to delineate different groups containing the majority of
223 single-, mixed- and non-SNVs, respectively. The X-axis represents the nucleotide position along the
224 respective reference genomes. The Y-axis represents the frequency of each SNV from NGS results.
225

226 To investigate the occurrence, distribution and persistency of SNVs over time in the F4-c1
227 sample extracts, SNVs from 120 to 1200 dpi were compared to those seen in the samples from the
228 earliest time point available (62 dpi). For each sample, there were 72-146 SNVs called by NGS with a
229 frequency >2% (Figure 2). Since the possibility for a NGS SNV with a frequency less than 35% to be
230 confirmed as a non-SNV by pyrosequencing was 89.1% based on our current model, and to make the
231 list more concise and clear, only the SNVs with frequencies > 10% (a total of 442 SNVs) were included
232 in the analysis (Supplementary Table 2). Each SNV had a Phred quality score >30, and the average
233 coverage ranged from 51-2558 x, except for the SNVs (single-SNV) at 7393 and 7417 nt positions in
234 996 and 1200 dpi samples. These SNVs had a coverage of 42, 22, 47 and 34x, respectively, but were
235 still higher than the requirement of an average depth of 15x for detection of "homozygous" SNV
236 (single-SNV) [35, 36]. All the SNVs were further predicted as either (182 out of 442 = 41%) single-, (93
237 out of 442 = 21%) mixed-, or (167 out of 442 = 38%) non-SNVs based on their NGS frequencies
238 (Supplementary Table 2). As summarized in Figure 3 (predicted non-SNVs were not included), (i)
239 SNVs were detected across the whole genome, including regions of UTRs, structural proteins and
240 non-structural proteins; (ii) a SNV detected at a nucleotide position from an early time point could
241 be persistently present in the samples from later time points; (iii) both mixed-SNVs (intra-host) and
242 single-SNV (inter-host) at a position were detected in samples from each time point; (iv) a majority
243 of the mixed (intra-host) SNVs from earlier time points would become single-SNV (inter-host) in later
244 time points, with a few of exceptions, such as the ones at nucleotide positions of 3005 and 4209; (v)
245 the number of SNVs increased in samples starting from 600-dpi, which was also shown in Figure 4;
246 (vi) SNVs from 62 nucleotide positions along the genome were detected and identified, based on the
247 model in the current study. Further analysis found that 12 out of these 62 SNVs were noncoding
248 SNVs, and the remaining 50 SNVs fell inside the protein-coding region (Supplementary Table 2).
249 Among these 50 SNVs in the coding region, 39 of them were synonymous, and only 11 of them were
250 nonsynonymous which resulted a change in the amino acid.
251

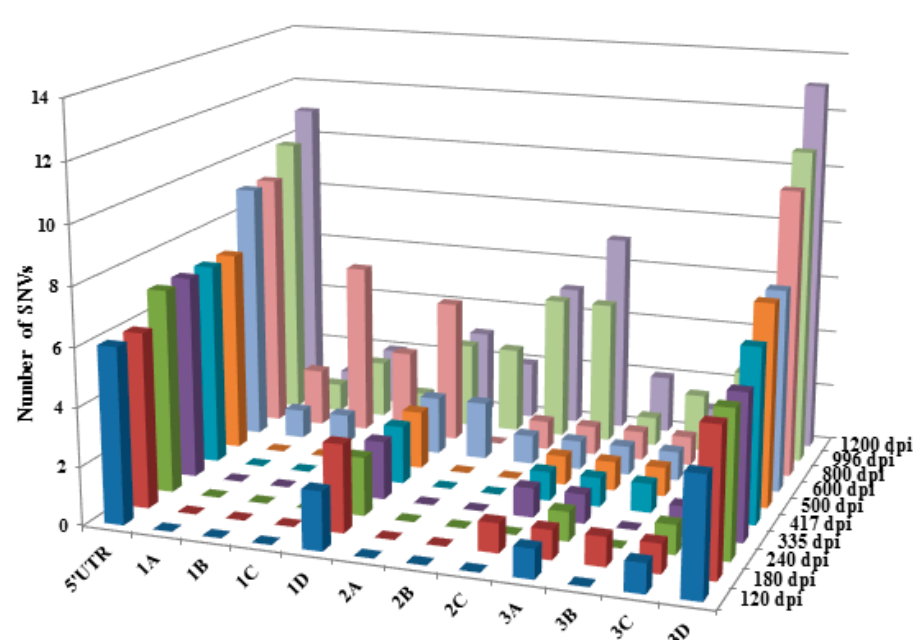


252
253
254
255
256
257

Figure 2. Distribution of single nucleotide variants across the F4-C1 genome at different timepoints. Each dot represents each SNV identified by NGS at the nucleotide position along the mapped reference sequence of F4-C1 genome at 62 dpi (x-axis) with its variant frequency (y-axis) at that position. Only those variants with a frequency > 2% are represented in the graphs.



258
 259 **Figure 3. SNVs in F4-c1 samples over time post-infection identified by NGS and predicted as**
 260 **intra- or inter-host variants based on the NGS frequency model.** SNVs were detected from each
 261 time point 120 to 1200 dpi (represented at different colors) against 62 dpi F4-C1 RNA sample, and
 262 variant frequencies determined and assignment as intra-, inter- or non-SNV variants as listed in
 263 Supplemental Table 2. Each triangle represents one SNV called by NGS and predicted as a single-
 264 SNV, and each circle represents one SNV called by NGS and predicted as mixed-SNVs. The X-axis
 265 represents the nucleotide position along the mapped reference sequence of F4-C1 genome at 62 dpi.
 266 Orange lines in the top panel represented various regions along the HAV genome: 5'-UTR (1-734 nt),
 267 capsid proteins 1A to 1D (735-3107 nt), non-structural proteins 2A to 3D (3708-7415 nt). 2C: ATPase
 268 (predicted); 3B: VPg; 3C: Protease; 3D: RNA-dependent RNA polymerase.
 269



271 **Figure 4. Distribution of SNVs along the HAV genome in F4-c1 samples.** SNVs in F4-C1
272 samples were detected from each time point 120 to 1200 dpi (represented as different colors)
273 against 62 dpi. X-axis represents different regions (not in proportion) along the mapped
274 reference sequence of F4-C1 genome at 62 dpi. Y-axis represents the number of SNVs in
275 each region. Z-axis represents the different time points at days post infection.
276

277

4. Discussion

278 For virologists working with foodborne viruses, achieving strain identification/ discrimination
279 at the level of single nucleotide differences/point mutations with a concomitant level of confidence
280 assigned to those differences remains an important goal. This level of discrimination would greatly
281 aid in not only strain identification, but also in outbreak investigation, regulatory surveillance, and
282 perhaps source attribution. Indeed, tracking virus strains by as few as one nucleotide variation could
283 be accomplished by whole genome sequencing. However, accurate identification of SNVs is
284 challenged by errors generated during NGS. Error reduction could be achieved by various strategies,
285 such as increasing the depth of reads coverage [37], or developing and improving bioinformatic tools
286 for data analysis and error identification, particularly for nucleotide variation [29, 38, 39]. In this
287 study, in addition to ensuring the high depth of coverage for the SNVs, we employed pyrosequencing
288 for the SNV confirmation.

289 The results showed (supplementary table 2) that some SNVs were repeatedly detected in a series
290 of F4-C1 samples by NGS, but not confirmed by pyrosequencing. For example, a SNV at nucleotide
291 position 1185 was called at 335 to 600 dpi with the frequency < 29.7%, then disappeared at later time
292 points. The explanations for this observation could be: (1) it was a random and/or repetitive NGS
293 error in SNV identification rather than a real variation, or (2) it was a real SNV at early time points,
294 but the mutation rate was lower than the pyrosequencing detection sensitivity (~5% allele frequency),
295 and thus it could not be confirmed. Additional explanation for the absence of this SNV at later time
296 points might be a result of negative selection. The latter interpretation is supported by another
297 observation in our study. For example, the SNV at nucleotide position 1348 was repeatedly called
298 from 417 to 1200 dpi by NGS with various frequencies. According to our NGS frequency model,
299 pyrosequencing would confirm it as a non-SNV at 417 and 500 dpi (NGS frequencies of 10.8% and
300 17.6%), a mixed-SNVs at 600 and 800 dpi (NGS frequencies of 51.1% and 40.7%), and a single-SNV at
301 996 and 1200 dpi (NGS frequencies of 87.1% and 86.6%). The possibility would be a real variation at
302 this position started from 417-dpi with a very low mutation frequency, then became the major and
303 eventually the dominant type due to the positive selection. Similarly, the SNVs called by NGS with
304 lower frequencies from earlier time points also occurred at other positions. These single nucleotide
305 mutations either were eliminated or became single-SNV SNVs at later time points, likely due to
306 different selective pressures on the replication and maintenance of the viral genome population.

307 It should be noted that only 12 out of 17 (70.6%) SNVs with NGS frequencies ranging between
308 35 to 70% were confirmed as mixed-SNVs by pyrosequencing and included in the current study.
309 Thus, for this specific model, a mixed-SNVs type of SNV was predicted with only a 70.6% probability
310 to be validated by pyrosequencing. Taking the small sample size ($n = 17$) into account, we believed
311 that when a new model is re-created, the SNV detection accuracy and the power of the model based
312 on the NGS frequencies could increase by increasing the sample number (the cutting-off frequency
313 % between groups could be altered accordingly), especially for the mixed-SNVs group.

314 It has been commonly believed that the 5'- and 3'-UTRs of HAV are highly conserved regions
315 [40, 41], and the coding region usually exhibits a high genetic diversity [42, 43]. Indeed, our results
316 obtained from the stool sample extract demonstrated that all seven confirmed SNVs fell within the
317 polyprotein coding region and with only one SNV (at position 2864 nt) located in the VP1-P2A
318 junction region. These results are consistent with the previous finding that, besides the VP1-P2A
319 junction, other regions across the genome also display nucleotide variability [19]. Interestingly, our
320 results of the cultured F4-C1 samples indicated that SNVs are distributed along the whole genome,
321 in both UTRs and coding regions. In fact, the more extensive nucleotide variants were observed in
322 both 5'-end (5'-UTR) and 3'-end (3D regions, RNA polymerase), compared with other individual
323 coding region (Figure 4). Previous studies demonstrated that the 5' proximal regions of uncapped
324 genome of picornaviruses have an internal ribosome entry site (IRES) and are involved in translation
325 as well as RNA synthesis [44, 45]. In addition, a stem-loop structure predicted in the 5' proximal
326 region of red clover necrotic mosaic virus played important host-dependent roles in both translation
327 and RNA stability [44]. Thus, the diverse structure of the 5' proximal region of the positive-sense
328 single-stranded RNA viruses is one of the strategies of the viruses to exploit host resources to perform

329 their own preferential translation or proper translation regulation [46, 47]. In the current study, the
330 pattern of SNV distribution between the wild-type stool sample and cultured F4-c1 samples differed
331 from each other. More genetic variations in HAV 5'-UTR, in combination with the 3D region
332 variations (RNA polymerase), might play roles for the virus translation, rapid proliferation and
333 culture adaptation in FRhK4 cells.

334 The original clone 1 strain that infected the FRhK4 cells, and samples from earlier time points
335 prior to 62 dpi were unavailable for inclusion in this investigation. Therefore, HAV evolution, amino
336 acid function change and mutation rate are beyond the extent of this study.

337 In summary, our study identified inter- and intra-host variants of HAV in different
338 environments and demonstrated the co-existence of inter- and intra-host variants both in the clinical
339 specimen and under laboratory culture conditions. Our findings of intra-host variants from the
340 clinical sample demonstrated the presence of multi-viral RNAs in a single infected individual. This
341 is significantly important for the discrimination of strains at the SNV level, outbreak investigations,
342 and source attribution. In other words, if more than one HAV molecule with only a few nucleotide
343 differences are detected from one food item, it could be from multiple contamination sources, but the
344 possibility of a single contamination source should not be excluded, and thereby further investigation
345 is needed. Additionally, the detection of HAV genetic variability using NGS, which is likely more
346 sensitive than traditional pyrosequencing, has improved our understanding of the basis controlling
347 on intra- and inter-host population dynamics. As such, the fate of mutations could be determined by
348 different selective pressures. A minority mutation, starting and maintaining at a low frequency, may
349 either be eliminated as the result of negative selection, or become a major type through positive
350 selection. Our study also suggested that whole-genome sequencing could potentially provide a
351 valuable approach to the studies, not only in HAV but also in other viruses, for the accurate
352 identification and source attribution at SNV level.

353 **Supplementary Materials:** The following are available online, Inter- and intra-host nucleotide variations of
354 hepatitis A virus in culture and clinical samples detected by next-generation sequencing. Figure S1: the
355 representative pyrogram of the heterozygosities. Table S1 (a) initial PCR primers for amplicons, (b) sequencing
356 primers for pyrosequencing. Table S2: summary of F4-c1 variants called by NGS from multiple timepoints
357 against 62-dpi.

358 **Author Contributions:** Zhihui Yang designed the study. Mark Mammel designed the primers for the
359 pyrosequencing assay and analyzed the pyrosequencing data. Diana Ngo and Michael Kulka generated the
360 FRhK-4 cell line persistently infected with HAV clone 1. Zhihui Yang performed the experiments, analyzed the
361 data, and wrote the paper; Chris Whitehouse and Michael Kulka supervised and revised the paper. All authors
362 discussed the results and contributed to the final manuscript. All authors approved the manuscript before it was
363 submitted by the corresponding author.

364 **Acknowledgments:** The authors would like to thank Marianna Solomotis for reviewing the manuscript.

365 **Conflicts of Interest:** The authors declare no conflict of interest.

366 **References**

- 368 1. Yang, Z.; Mammel, M.; Papafragkou, E.; Hida, K.; Elkins, C. A.; Kulka, M., Application of
369 next generation sequencing toward sensitive detection of enteric viruses isolated from
370 celery samples as an example of produce. *Int J Food Microbiol* **2017**, *261*, 73-81.
- 371 2. Kunkel, T. A., Exonucleolytic proofreading. *Cell* **1988**, *53*, (6), 837-840.
- 372 3. Vaughan, G.; Goncalves Rossi, L. M.; Forbi, J. C.; de Paula, V. S.; Purdy, M. A.; Xia, G.;
373 Khudyakov, Y. E., Hepatitis A virus: host interactions, molecular epidemiology and
374 evolution. *Infect Genet Evol* **2014**, *21*, 227-43.
- 375 4. Domingo, E.; Sheldon, J.; Perales, C., Viral quasispecies evolution. *Microbiol Mol Biol Rev*
376 **2012**, *76*, (2), 159-216.

377 5. Nowak, M. A., What is a quasispecies? *Trends Ecol Evol* **1992**, 7, (4), 118-21.

378 6. Barik, S.; Das, S.; Vikalo, H., QSdpR: Viral quasispecies reconstruction via correlation
379 clustering. *Genomics* **2017**.

380 7. Scallan, E.; Hoekstra, R. M.; Angulo, F. J.; Tauxe, R. V.; Widdowson, M. A.; Roy, S. L.; Jones,
381 J. L.; Griffin, P. M., Foodborne illness acquired in the United States--major pathogens.
382 *Emerging infectious diseases* **2011**, 17, (1), 7-15.

383 8. Werzberger, A.; Mensch, B.; Kuter, B.; Brown, L.; Lewis, J.; Sitrin, R.; Miller, W.; Shouval,
384 D.; Wiens, B.; Calandra, G.; et al., A controlled trial of a formalin-inactivated hepatitis A
385 vaccine in healthy children. *N Engl J Med* **1992**, 327, (7), 453-7.

386 9. Innis, B. L.; Snitbhan, R.; Kunasol, P.; Laorakpongse, T.; Poopatanakool, W.; Kozik, C. A.;
387 Suntayakorn, S.; Suknuntapong, T.; Safary, A.; Tang, D. B.; et al., Protection against
388 hepatitis A by an inactivated vaccine. *JAMA* **1994**, 271, (17), 1328-34.

389 10. Lanini, S.; Minosse, C.; Vairo, F.; Garbuglia, A.; Di Bari, V.; Agresta, A.; Rezza, G.; Puro, V.;
390 Pendenza, A.; Loffredo, M. R.; Scognamiglio, P.; Zumla, A.; Panella, V.; Ippolito, G.;
391 Capobianchi, M. R., A large ongoing outbreak of hepatitis A predominantly affecting
392 young males in Lazio, Italy; August 2016 - March 2017. *PLoS one* **2017**, 12, (11), e0185428.

393 11. Shin, E.; Kim, J. S.; Oh, K. H.; Oh, S. S.; Kwon, M.; Kim, S.; Park, J.; Kwak, H. S.; Chung, G.
394 T.; Kim, C. J.; Kim, J., A waterborne outbreak involving hepatitis A virus genotype IA at a
395 residential facility in the Republic of Korea in 2015. *Journal of clinical virology : the official
396 publication of the Pan American Society for Clinical Virology* **2017**, 94, 63-66.

397 12. Bruni, R.; Taffon, S.; Equestre, M.; Cella, E.; Lo Presti, A.; Costantino, A.; Chionne, P.;
398 Madonna, E.; Golkocheva-Markova, E.; Bankova, D.; Ciccozzi, M.; Teoharov, P.;
399 Ciccaglione, A. R., Hepatitis a virus genotypes and strains from an endemic area of Europe,
400 Bulgaria 2012-2014. *BMC Infect Dis* **2017**, 17, (1), 497.

401 13. Collier, M. G.; Khudyakov, Y. E.; Selvage, D.; Adams-Cameron, M.; Epson, E.; Cronquist,
402 A.; Jervis, R. H.; Lamba, K.; Kimura, A. C.; Sowadsky, R.; Hassan, R.; Park, S. Y.; Garza, E.;
403 Elliott, A. J.; Rotstein, D. S.; Beal, J.; Kuntz, T.; Lance, S. E.; Dreisch, R.; Wise, M. E.; Nelson,
404 N. P.; Suryaprasad, A.; Drobeniuc, J.; Holmberg, S. D.; Xu, F., Outbreak of hepatitis A in the
405 USA associated with frozen pomegranate arils imported from Turkey: an epidemiological
406 case study. *The Lancet. Infectious diseases* **2014**, 14, (10), 976-81.

407 14. Costa, A. M.; Amado, L. A.; Paula, V. S. d., Detection of replication-defective hepatitis A
408 virus based on the correlation between real-time polymerase chain reaction and ELISA in
409 situ results. *Memórias do Instituto Oswaldo Cruz* **2013**, 108, 36-40.

410 15. Costa-Mattioli, M.; Cristina, J.; Romero, H.; Perez-Bercof, R.; Casane, D.; Colina, R.; Garcia,
411 L.; Vega, I.; Glikman, G.; Romanowsky, V.; Castello, A.; Nicand, E.; Gassin, M.; Billaudel, S.;
412 Ferré, V., Molecular Evolution of Hepatitis A Virus: a New Classification Based on the
413 Complete VP1 Protein. *Journal of Virology* **2002**, 76, (18), 9516-9525.

414 16. Feinstone, S. M.; Kapikian, A. Z.; Purceli, R. H., Hepatitis A: detection by immune electron
415 microscopy of a viruslike antigen associated with acute illness. *Science* **1973**, 182, (4116),
416 1026-8.

417 17. Robertson, B. H.; Jansen, R. W.; Khanna, B.; Totsuka, A.; Nainan, O. V.; Siegl, G.; Widell, A.;
418 Margolis, H. S.; Isomura, S.; Ito, K.; Ishizu, T.; Moritsugu, Y.; Lemon, S. M., Genetic

419 relatedness of hepatitis A virus strains recovered from different geographical regions.
420 *Journal of General Virology* 1992, 73, (6), 1365-1377.

421 18. Brown, E. A.; Jansen, R. W.; Lemon, S. M., Characterization of a simian hepatitis A virus
422 (HAV): antigenic and genetic comparison with human HAV. *J Virol* 1989, 63, (11), 4932-7.

423 19. Forbi, J. C.; Esona, M. D.; Agwale, S. M., Molecular characterization of hepatitis A virus
424 isolates from Nigeria. *Intervirology* 2013, 56, (1), 22-6.

425 20. Costa-Mattioli, M.; Domingo, E.; Cristina, J., Analysis of sequential hepatitis A virus strains
426 reveals coexistence of distinct viral subpopulations. *The Journal of general virology* 2006, 87,
427 (Pt 1), 115-8.

428 21. Y., S.; C.R., G.; B., M.; D., R.; D., S.; J., N.; E., R.; F.H., P., Hepatitis A virus genetic diversity
429 in Venezuela: Exclusive circulation of subgenotype IA and evidence of quasispecies
430 distribution in the isolates. *Journal of medical virology* 2010, 82, (11), 1829-1834.

431 22. Sanchez, G.; Bosch, A.; Gómez-Mariano, G.; Domingo, E.; Pintó, R., *Evidence for quasispecies*
432 *distributions in the human Hepatitis A virus genome*. 2003; Vol. 315, p 34-42.

433 23. Vaughan, G.; Xia, G.; Forbi, J. C.; Purdy, M. A.; Rossi, L. M.; Spradling, P. R.; Khudyakov, Y.
434 E., Genetic relatedness among hepatitis A virus strains associated with food-borne
435 outbreaks. *PLoS one* 2013, 8, (11), e74546.

436 24. Yang, Z.; Leonard, S. R.; Mammel, M. K.; Elkins, C. A.; Kulka, M., Towards next-generation
437 sequencing analytics for foodborne RNA viruses: Examining the effect of RNA input
438 quantity and viral RNA purity. *J Virol Methods* 2016, 236, 221-30.

439 25. Goswami, B. B.; Kulka, M.; Ngo, D.; Cebula, T. A., Apoptosis induced by a cytopathic
440 hepatitis A virus is dependent on caspase activation following ribosomal RNA degradation
441 but occurs in the absence of 2'-5' oligoadenylate synthetase. *Antiviral research* 2004, 63, (3),
442 153-66.

443 26. Kulka, M.; Calvo, M. S.; Ngo, D. T.; Wales, S. Q.; Goswami, B. B., Activation of the 2'-
444 5'OAS/RNase L pathway in CVB1 or HAV/18f infected FRhK-4 cells does not require
445 induction of OAS1 or OAS2 expression. *Virology* 2009, 388, (1), 169-184.

446 27. Wales, S. Q.; Ngo, D.; Hida, K.; Kulka, M., Temperature and density dependent induction
447 of a cytopathic effect following infection with non-cytopathic HAV strains. *Virology* 2012,
448 430, (1), 30-42.

449 28. Bravo, H. C.; Irizarry, R. A., Model-based quality assessment and base-calling for second-
450 generation sequencing data. *Biometrics* 2010, 66, (3), 665-74.

451 29. Beerewinkel, N.; Gunthard, H. F.; Roth, V.; Metzner, K. J., Challenges and opportunities in
452 estimating viral genetic diversity from next-generation sequencing data. *Frontiers in*
453 *microbiology* 2012, 3, 329.

454 30. Hayford, A. E.; Mammel, M. K.; Lacher, D. W.; Brown, E. W., Single nucleotide
455 polymorphism (SNP)-based differentiation of *Shigella* isolates by pyrosequencing. *Infect*
456 *Genet Evol* 2011, 11, (7), 1761-8.

457 31. Janecek, E.; Streichan, S.; Strube, C., SNP-based real-time pyrosequencing as a sensitive and
458 specific tool for identification and differentiation of *Rickettsia* species in *Ixodes ricinus*
459 ticks. *BMC Infect Dis* 2012, 12, (261), 1471-2334.

460 32. Jones, C. H.; Ruzin, A.; Tuckman, M.; Visalli, M. A.; Petersen, P. J.; Bradford, P. A.,
461 Pyrosequencing using the single-nucleotide polymorphism protocol for rapid

462 determination of TEM- and SHV-type extended-spectrum beta-lactamases in clinical
463 isolates and identification of the novel beta-lactamase genes blaSHV-48, blaSHV-105, and
464 blaTEM-155. *Antimicrobial agents and chemotherapy* **2009**, 53, (3), 977-86.

465 33. Satkoski, J. A.; Malhi, R.; Kanthaswamy, S.; Tito, R.; Malladi, V.; Smith, D., Pyrosequencing
466 as a method for SNP identification in the rhesus macaque (*Macaca mulatta*). *BMC genomics*
467 **2008**, 9, 256.

468 34. Pu, D.; Pan, R.; Liu, W.; Xiao, P., Quantitative analysis of single-nucleotide polymorphisms
469 by pyrosequencing with di-base addition. *Electrophoresis* **2017**, 38, (6), 876-885.

470 35. Sims, D.; Sudbery, I.; Ilott, N. E.; Heger, A.; Ponting, C. P., Sequencing depth and coverage:
471 key considerations in genomic analyses. *Nature reviews. Genetics* **2014**, 15, (2), 121-32.

472 36. Bentley, D. R.; Balasubramanian, S.; Swerdlow, H. P.; Smith, G. P.; Milton, J.; Brown, C. G.;
473 Hall, K. P.; Evers, D. J.; Barnes, C. L.; Bignell, H. R.; Boutell, J. M.; Bryant, J.; Carter, R. J.;
474 Keira Cheetham, R.; Cox, A. J.; Ellis, D. J.; Flatbush, M. R.; Gormley, N. A.; Humphray, S. J.;
475 Irving, L. J.; Karbelashvili, M. S.; Kirk, S. M.; Li, H.; Liu, X.; Maisinger, K. S.; Murray, L. J.;
476 Obradovic, B.; Ost, T.; Parkinson, M. L.; Pratt, M. R.; Rasolonjatovo, I. M.; Reed, M. T.;
477 Rigatti, R.; Rodighiero, C.; Ross, M. T.; Sabot, A.; Sankar, S. V.; Scally, A.; Schroth, G. P.;
478 Smith, M. E.; Smith, V. P.; Spiridou, A.; Torrance, P. E.; Tzonev, S. S.; Vermaas, E. H.;
479 Walter, K.; Wu, X.; Zhang, L.; Alam, M. D.; Anastasi, C.; Aniebo, I. C.; Bailey, D. M.;
480 Bancarz, I. R.; Banerjee, S.; Barbour, S. G.; Baybayan, P. A.; Benoit, V. A.; Benson, K. F.;
481 Bevis, C.; Black, P. J.; Boodhun, A.; Brennan, J. S.; Bridgman, J. A.; Brown, R. C.; Brown, A.
482 A.; Buermann, D. H.; Bundu, A. A.; Burrows, J. C.; Carter, N. P.; Castillo, N.; Chiara, E. C.
483 M.; Chang, S.; Neil Cooley, R.; Crake, N. R.; Dada, O. O.; Diakoumakos, K. D.; Dominguez-
484 Fernandez, B.; Earnshaw, D. J.; Egbujor, U. C.; Elmore, D. W.; Etchin, S. S.; Ewan, M. R.;
485 Fedurco, M.; Fraser, L. J.; Fuentes Fajardo, K. V.; Scott Furey, W.; George, D.; Gietzen, K. J.;
486 Goddard, C. P.; Golda, G. S.; Granieri, P. A.; Green, D. E.; Gustafson, D. L.; Hansen, N. F.;
487 Harnish, K.; Haudenschild, C. D.; Heyer, N. I.; Hims, M. M.; Ho, J. T.; Horgan, A. M.;
488 Hoschler, K.; Hurwitz, S.; Ivanov, D. V.; Johnson, M. Q.; James, T.; Huw Jones, T. A.; Kang,
489 G. D.; Kerelska, T. H.; Kersey, A. D.; Khrebtukova, I.; Kindwall, A. P.; Kingsbury, Z.;
490 Kokko-Gonzales, P. I.; Kumar, A.; Laurent, M. A.; Lawley, C. T.; Lee, S. E.; Lee, X.; Liao, A.
491 K.; Loch, J. A.; Lok, M.; Luo, S.; Mammen, R. M.; Martin, J. W.; McCauley, P. G.; McNitt, P.;
492 Mehta, P.; Moon, K. W.; Mullens, J. W.; Newington, T.; Ning, Z.; Ling Ng, B.; Novo, S. M.;
493 O'Neill, M. J.; Osborne, M. A.; Osnowski, A.; Ostadan, O.; Paraschos, L. L.; Pickering, L.;
494 Pike, A. C.; Pike, A. C.; Chris Pinkard, D.; Pliskin, D. P.; Podhasky, J.; Quijano, V. J.; Raczy,
495 C.; Rae, V. H.; Rawlings, S. R.; Chiva Rodriguez, A.; Roe, P. M.; Rogers, J.; Rogert
496 Bacigalupo, M. C.; Romanov, N.; Romieu, A.; Roth, R. K.; Rourke, N. J.; Ruediger, S. T.;
497 Rusman, E.; Sanches-Kuiper, R. M.; Schenker, M. R.; Seoane, J. M.; Shaw, R. J.; Shiver, M. K.;
498 Short, S. W.; Sizto, N. L.; Sluis, J. P.; Smith, M. A.; Ernest Sohna Sohna, J.; Spence, E. J.;
499 Stevens, K.; Sutton, N.; Szajkowski, L.; Tregidgo, C. L.; Turcatti, G.; Vandevondrele, S.;
500 Verhovsky, Y.; Virk, S. M.; Wakelin, S.; Walcott, G. C.; Wang, J.; Worsley, G. J.; Yan, J.; Yau,
501 L.; Zuerlein, M.; Rogers, J.; Mullikin, J. C.; Hurles, M. E.; McCooke, N. J.; West, J. S.; Oaks, F.
502 L.; Lundberg, P. L.; Klenerman, D.; Durbin, R.; Smith, A. J., Accurate whole human genome
503 sequencing using reversible terminator chemistry. *Nature* **2008**, 456, (7218), 53-9.

504 37. Ajay, S. S.; Parker, S. C.; Abaan, H. O.; Fajardo, K. V.; Margulies, E. H., Accurate and
505 comprehensive sequencing of personal genomes. *Genome Res* **2011**, *21*, (9), 1498-505.

506 38. Beerenswinkel, N.; Zagordi, O., Ultra-deep sequencing for the analysis of viral populations.
507 *Current Opinion in Virology* **2011**, *1*, (5), 413-418.

508 39. Zagordi, O.; Klein, R.; Daumer, M.; Beerenswinkel, N., Error correction of next-generation
509 sequencing data and reliable estimation of HIV quasispecies. *Nucleic Acids Res* **2010**, *38*, (21),
510 7400-9.

511 40. Belalov, I. S.; Isaeva, O. V.; Lukashev, A. N., Recombination in hepatitis A virus: evidence
512 for reproductive isolation of genotypes. *The Journal of general virology* **2011**, *92*, (Pt 4), 860-72.

513 41. Desbois, D.; Couturier, E.; Mackiewicz, V.; Graube, A.; Letort, M. J.; Dussaix, E.; Roque-
514 Afonso, A. M., Epidemiology and genetic characterization of hepatitis A virus genotype
515 IIA. *J Clin Microbiol* **2010**, *48*, (9), 3306-15.

516 42. Robertson, B. H.; Khanna, B.; Nainan, O. V.; Margolis, H. S., Epidemiologic patterns of
517 wild-type hepatitis A virus determined by genetic variation. *The Journal of infectious diseases*
518 **1991**, *163*, (2), 286-92.

519 43. Lee, H.; Jeong, H.; Yun, H.; Kim, K.; Kim, J. H.; Yang, J. M.; Cheon, D. S., Genetic analysis of
520 hepatitis A virus strains that induced epidemics in Korea during 2007-2009. *J Clin Microbiol*
521 **2012**, *50*, (4), 1252-7.

522 44. Sarawaneeyaruk, S.; Iwakawa, H.-o.; Mizumoto, H.; Murakami, H.; Kaido, M.; Mise, K.;
523 Okuno, T., Host-dependent roles of the viral 5' untranslated region (UTR) in RNA
524 stabilization and cap-independent translational enhancement mediated by the 3' UTR of
525 Red clover necrotic mosaic virus RNA1. *Virology* **2009**, *391*, (1), 107-118.

526 45. Svitkin, Y. V.; Imataka, H.; Khaleghpour, K.; Kahvejian, A.; Liebig, H. D.; Sonenberg, N.,
527 Poly(A)-binding protein interaction with eIF4G stimulates picornavirus IRES-dependent
528 translation. *RNA* **2001**, *7*, (12), 1743-52.

529 46. Pestova, T. V.; Kolupaeva, V. G., The roles of individual eukaryotic translation initiation
530 factors in ribosomal scanning and initiation codon selection. *Genes Dev* **2002**, *16*, (22), 2906-
531 22.

532 47. Kozak, M., The scanning model for translation: an update. *J Cell Biol* **1989**, *108*, (2), 229-41.